

A theoretical model of the manufacture of reaction-bonded silicon nitride with particular emphasis on the effect of ambient reaction temperature and compact size

G. S. HUGHES*, C. MCGREAVY†, J. H. MERKIN*

**Department of Applied Mathematical Studies and †Department of Chemical Engineering, University of Leeds, Leeds, UK*

An analysis of the exothermic, irreversible silicon–nitrogen reaction, based on the particle–pellet model, is presented using mixed type boundary conditions to represent external resistances. The mathematical model incorporates a sharp “cut-off” in the reaction and takes into account its transient behaviour. The resulting system of partial differential equations is solved numerically using an explicit finite difference scheme. The effects of varying the ambient reaction temperature and compact size on the temperature distribution inside the nitriding compact and on the solid product formation rate, are examined. The results obtained are in acceptable agreement with previous experimental research by other workers, which illustrates how the model adequately represents the silicon–nitrogen reaction.

An investigatory report on the validity of the Arrhenius equation for determining the thermal activation energy of this reaction is also presented.

a	= characteristic dimensions of the compact, m .	$r(C, T)$	= reaction rate per unit area, $\text{kg m}^{-2} \text{sec}^{-1}$.
C	= concentration of the gas within the compact, mol m^{-3} .	r_p	= mean particle size, m .
C_A	= molar concentration of the product in the compact, mol m^{-3} .	s_g	= specific area of the compact, $7.142 \times 10^2 \text{ m}^2 \text{ kg}^{-1}$.
C_{AO}	= maximum concentration of the product, $1.6 \times 10^4 \text{ mol m}^{-3}$.	T	= absolute temperature within the compact, K .
C_f	= concentration of the gas surrounding the compact, mol m^{-3} .	T_c	= temperature at the centre of the compact, K .
C_p	= specific heat of solid reactant, $1250 \text{ J kg}^{-1} \text{ K}^{-1}$.	T_f	= initial and surrounding temperature, K .
D_e	= effective diffusion coefficient, $2 \times 10^{-6} \text{ m}^2 \text{ sec}^{-1}$.	T_s	= temperature at the surface of the compact, K .
E	= activation energy of reaction, $5.5 \times 10^5 \text{ J mol}^{-1}$.	t	= time, sec .
ΔH	= heat of reaction, $-7.5 \times 10^5 \text{ J mol}^{-1}$.	u	= dimensionless concentration of the gas in the compact.
h	= heat transfer coefficient, $\text{W m}^{-2} \text{ K}^{-1}$.	U_A	= C_A/C_{AO} .
K_e	= effective thermal conductivity, $6.6 \text{ W m}^{-1} \text{ K}^{-1}$.	V^*	= dimensionless space.
$\partial/\partial n$	= derivative normal to the surface of the compact.	ν	= dimensionless temperature in the compact.
		X	= conversion factor, defined by Equation 7.

x = dimensionless space variable within the compact.
 ϵ = void fraction of the compact, $\times 0.4$.

ρ_b = bulk density of the compact, 1400 kg m^{-3} .
 τ = dimensionless time.

1. Introduction

Interest in reaction-bonded silicon nitride as a high temperature engineering ceramic has grown over the past twenty years. This has stimulated numerous detailed studies of the system and the nitridation mechanisms involved, the majority of which are reviewed in a recent paper by Moulson [1]. Although these extensive investigations have resulted in considerable insight into some of the significant processes involved, they are still far from complete. The reason lies in the fact that the overall mechanism is undoubtedly a very complex one. Failure to take into account the many factors which complicate the process often invalidates direct comparison of experimental results between different workers. This partly accounts for the diverse interpretations which are presented in the literature. A prime example being, the sensitivity of the reaction to small amounts of impurities in the reactants, which are frequently ignored [2]. It is the authors' view that the development of a mathematical model is necessary to ascertain the basic principles of the reaction. The aim in developing such a model is three-fold. Firstly, it is hoped that the model will highlight those physical parameters which are needed for a full description of the process, and consequently lead to experimental work for their accurate determination. Secondly, a reliable model of the nitridation process can enable different nitriding strategies to be readily evaluated without the use of costly experimental procedures and the optimum one can then be suggested for a given laboratory or industrial schedule. Thirdly, the model will also enable the relevance of the various empirical formulae presented in the past to be investigated.

Several mathematical models have already been presented in the past for non-catalytic gas-solid reactions, the majority of which use various simplifying assumptions. For example, the frequently used isothermal approximation is obviously inappropriate to the silicon-nitrogen reaction, since an important feature of this reaction is its highly exothermic nature ($\Delta H = -0.75 \text{ MJ mol}^{-1}$). The resultant temperature gradients, influence the rate of reaction and this suggests that the transient state must be considered. Also the diffusion of both heat and nitrogen with-

in the compact is important and the appearance of concentration and temperature gradients invites the use of a particle-pellet model. This kind of model has previously been used by Sampath, Ramachandran and Hughes [3, 4], though for a completely different reaction, and the present model differs from theirs in several important respects.

In the research described in the present paper particular emphasis has been placed on investigating the temperature distributions inside the nitriding compact, and how these change with ambient reaction temperature and compact size. Consideration has also been given to the effect this has on the overall reaction-bonding process. The majority of this work was instigated by experimental research carried out by Atkinson, Leatt and Moulson [6].

2. Model formulation and equations

In attempting to construct a mathematical model to represent a physical system, certain simplifying assumptions have to be made, whilst still retaining the more essential features of the process. The following assumptions are made for the present model.

(a) The diffusion and reaction processes within the compact can be described by effective overall parameters, which remain invariant during the reaction.

(b) The chemical reaction is of the single, first order, irreversible type.

(c) The silicon and nitrogen are pure reactants, in that the effects of impurities on the reaction are ignored.

A sketch of the structural model is shown in Fig. 1. The slab of thickness $2a$ consists of fine particles of mean radius r_p .

General material and heat balances on both the gas and solid reactants give rise to the following partial differential equations [7].

$$\epsilon \frac{\partial C}{\partial t} = D_e \nabla^2 C - \rho_b S_g r(C, T) \quad (1)$$

$$\rho_b C_p \frac{\partial T}{\partial t} = K_e \nabla^2 T + \rho_b S_g (-\Delta H) r(C, T). \quad (2)$$

If C_A is the amount of nitride formed at a given

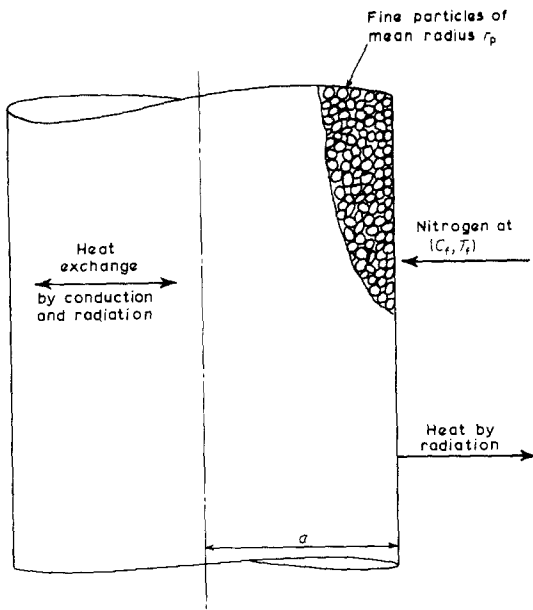
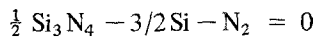


Figure 1 A sketch of the structural model.

point inside the compact then

$$C_A = \frac{1}{2} \int_0^t \rho_b S_g r(C, T) dt \quad (3)$$

where the reaction is given stoichiometrically by



The rate expression takes the form

$$r = CK_0 \exp(-E/RT), \quad C_A < C_{AO} \\ = 0, \quad C_A = C_{AO} \quad (4)$$

According to Mouslon [1] and Riley [8] in the silicon-nitrogen reaction, the silicon first vaporizes and then reacts with the nitrogen, depositing the solid product within the original pore structure giving rise to a microstructure which is quite different from that of the original compact. This suggests that a sharp cut-off in the reaction, when $C_A = C_{AO}$ as given by Equation 4, is more appropriate to this model rather than assuming that each particle which makes up the compact reacts as a "shrinking-core model" as in [3].

To complete the model a set of initial and boundary conditions are needed and to fix these the following nitridation strategy was assumed:- The compact of silicon powder is first heated to a constant temperature T_f , in a vacuum and nitrogen is introduced so that the compact is completely surrounded by gas at a constant concentration C_f . This gives the initial conditions

$$t = 0; C = 0, T = T_f \quad (5)$$

and the boundary conditions

$$C = C_f; K_e \frac{\partial T}{\partial n} = h(T_f - T) \quad (6)$$

These could easily be modified without affecting the basic model to account for different nitriding strategies.

Equations 1 to 6 are first non-dimensionalized by introducing the non-dimensional variables

$$u = C/C_f, \quad v = T/T_f, \quad \tau = D_e t/a^2 \epsilon,$$

$$U_A = C_A/C_{AO}$$

and then solved numerically for a plane geometry using an explicit finite difference scheme. The details of the method have already been presented by Hughes, McGreavy and Merkin [9] and Hughes [10] and can be directly referred to should the reader wish. The conversion factor $X(\tau)$ is defined as

$$X = \int_V \frac{U_A}{V^*} dV^* \quad (7)$$

Various investigations involving changing the ambient reaction temperature T_f , and the compact size are presented in the next section. In order to compare the different compact sizes, without reverting back to real time, the non-dimensional time scale for the 5 cm compact, $\tau(5 \text{ cm})$ is taken as a base and all times, τ , are rescaled according to

$$\tau(5 \text{ cm}) = \frac{\tau a^2}{6.25 \times 10^{-4}} \quad (8)$$

The Arrhenius equation from [5] is stated here for future reference

$$\frac{dX}{dt} = A \exp(-E/RT) \quad (9)$$

where dX/dt is the conversion rate.

3. Results and discussion

The majority of the data used in this report is taken from Mouslon [1] and Riley [8] and confirmed by various other sources [6, 11]. Where data are not directly available, theoretical estimates have to be made. Consequently the results that are presented in the next section can really only provide a qualitative description of the process. This stresses the important need for a more accurate experimental determination of the significant physical parameters used in the model.

The most difficult parameters to obtain information on are the effective diffusivity D_e , the specific area per unit volume of the pellet $\rho_b s_g$, the heat transfer coefficient h , and the effective thermal conductivity K_e . A value for D_e is estimated from Knudsen Flow using the Lorentz derivation [7], as the mean free path of nitrogen ($0.6 \mu\text{m}$ at 1400°C) will be large in comparison to the reported measured pore sizes [6, 11]. The value obtained is consistent with that used in other studies [3, 4]. Experimental evidence suggests that $\rho_b s_g$ can vary considerably between compacts so an average value is calculated with the particles being regarded as hard spheres. No experimental data is available for h . At the high temperatures involved heat transfer from the compact is mainly by radiation and consequently it is reasonable to use the Stefan–Boltzmann law [12]. Only theoretical estimates of K_e for silicon nitride are available [5], so this was used in conjunction with that for silicon, which is known, to obtain an average value for the reaction.

The nominal values of the system parameters are given in the nomenclature.

3.1. Investigation of the effect of different ambient temperatures

3.1.1. Temperature measurements

The maximum temperature rises observed at the centre and surface for different ambient temperatures are presented in Table I. The temperature rises shown for the 5 cm compact compare favourably with experimental results by Atkinson and Evans [5], where an average temperature rise of $25 \pm 4^\circ\text{C}$ at the centre was observed for ambient temperatures in the range 1290 to 1330°C . The average temperature rise for this model, over the same range, being 25°C . The temperature changes in the compact, from the experimental data, are

interpreted to be independent of ambient reaction temperature in this range, whereas the values obtained from this model, over an extended range, indicate a definite relationship between the two. Note that this is also the case here for compacts of different sizes.

Experimentally, it is difficult to measure these fractional temperature changes, at such high ambient temperatures, to any degree of accuracy, as there are many factors, such as radiation effects and the presence of thermocouples inside the compact, which can affect the measured temperature rise and are difficult to account for.

The temperature–time variation is shown in Fig. 2, for two different ambient temperatures, where T_c is the temperature at the centre of the compact and T_s the temperature at the surface. It can be seen that the largest temperature excess occurs in the centre, at the beginning of the reaction, and is subsequently followed by the compact cooling. If T_f is decreased the initial peak in the temperature becomes less pronounced. A similar temperature–time curve can be seen in [5].

Although the temperatures shown in Fig. 2 and Table I are calculated using a constant property model, recent work has shown that if the respective parameters are allowed to vary during the reaction, this will only alter the temperatures slightly and not affect the general results.

3.1.2. Solid conversion

The effect of varying the ambient temperature, T_f on the progress of conversion is shown in Fig. 3, where the conversion factor X is plotted against dimensionless time for the 5 cm compact.

Increasing T_f increases the rate of reaction, with each line becoming more curved, owing to the increased variation in the internal tempera-

TABLE I Maximum temperature excess (T_{max}) occurring at different ambient temperatures T_f for 5, 7 and 0.5 cm compact sizes

T_f ($^\circ\text{C}$)	5 cm		7 cm		0.5 cm	
	ΔT_{max} at centre ($^\circ\text{C}$)	ΔT_{max} at surface ($^\circ\text{C}$)	ΔT_{max} at centre ($^\circ\text{C}$)	ΔT_{max} at surface ($^\circ\text{C}$)	ΔT_{max} at centre ($^\circ\text{C}$)	ΔT_{max} at surface ($^\circ\text{C}$)
1370	62.9	39.5	66.0	41.2	4.9	4.4
1350	50.3	29.1	55.4	30.6	3.0	2.75
1330	36.9	20.0	45.7	22.8	1.9	1.7
1310	23.3	12.5	34.0	16.0	1.26	1.16
1290	14.0	7.5	22.3	10.4	0.74	0.68
1250	4.7	2.6	7.8	3.7	0.26	0.25

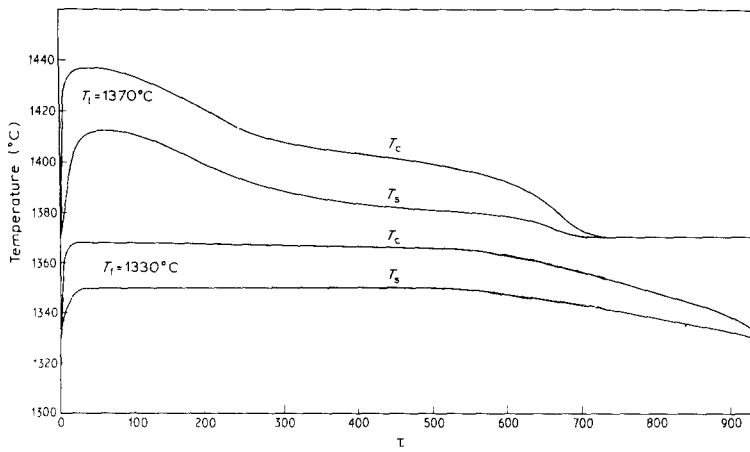


Figure 2 Temperature-time curves for a 5 cm compact.

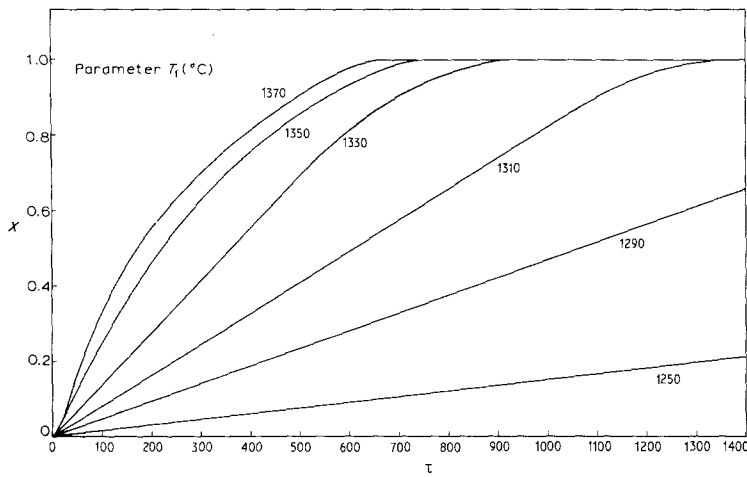


Figure 3 The effect of ambient temperature on the nitridation of 5 cm compacts.

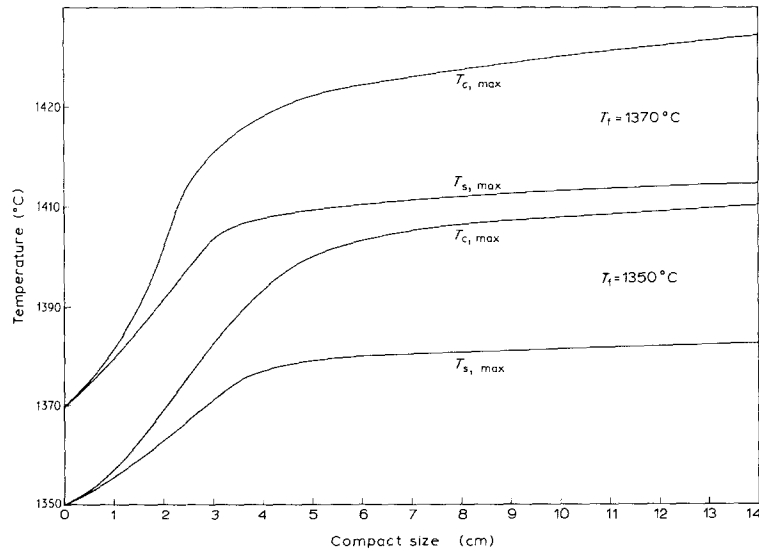


Figure 4 The effect of compact size on the maximum temperature attained at the centre $T_{c,max}$ and at the surface $T_{s,max}$ for $T_f = 1370^\circ\text{C}$ and $T_f = 1350^\circ\text{C}$.

ture as shown in Fig. 2. At $T_f = 1370^\circ\text{C}$, the reaction becomes slightly diffusion limited in that the nitrogen is being consumed at a faster rate than it can be replenished. Subsequently the rate of reaction in the centre soon decelerates owing to the reduction in available nitrogen, eventually decelerating below that for the $T_f = 1350^\circ\text{C}$ reaction. This graph is comparable with experimental results obtained by Atkinson, Leatt and Moulson [6] using a 3 cm diameter compact.

3.2. Investigation of the effect of different compact sizes

3.2.1. Temperature measurements

The temperature distribution has already been discussed for the 5 cm compact and Table I shows how the temperature rise increases and decreases throughout, for a large and small compact respectively. However, the temperature difference is not expected to increase indefinitely, and this can be seen in Fig. 4, where the maximum temperature attained at the centre T_c (max) and at the surface T_s (max) is plotted against compact size for two different values of T_f .

Fig. 5 shows that for increased compact size the amount of nitrogen reaching the centre decreases until there is virtually no reaction occurring there. At this point the contribution from the centre, to the temperature rise is negligible and the curve levels off. The area around the centre continues to react, and through conduction, T_c now becomes a measure of the neighbouring temperatures instead. If T_f is decreased, the size of the compact at which this occurs, increases slightly. This is a result of less reaction occurring throughout which enables more nitrogen to diffuse into the compact.

3.2.2. Solid conversion

The effect of compact size on the progress of conversion is shown in Table II and Figs. 6 and 7 where the latter are plots of the conversion factor X against a relative dimensionless time $\tau(5\text{ cm})$ for $T_f = 1370^\circ\text{C}$, and $T_f = 1330^\circ\text{C}$ respectively.

Figs. 6 and 7 show that as the compact size is increased the time for the compact to complete nitridation increases, which is to be expected. However, for very small compacts, less than 3 cm the total reaction time starts to increase again. Also on examination we note that the 0.5 cm and 1 cm compacts produce straight lines [2].

Table I illustrates the overall low excess temperatures that exist inside the 0.5 cm compact,

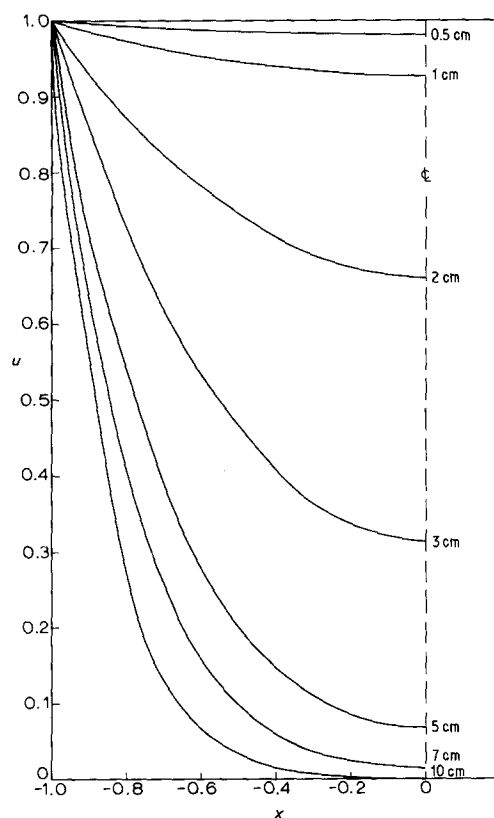


Figure 5 Comparison of concentration profiles for various compact sizes, at the same relative non-dimensional time $\tau(5\text{ cm}) = 28$, with $T_f = 1370^\circ\text{C}$.

together with an abundance of nitrogen, (see Fig. 5) this produces a very uniform product formation throughout, which accounts for the latter phenomenon above. Increasing the compact to 1 cm gives a higher temperature rise, see Fig. 4, which increases the reaction rate, and with the nitrogen still remaining abundant throughout, this reduces the total reaction time. The reaction at this point has thus become solely temperature dependent. Hence for small compacts

TABLE II Reaction time period for various compact sizes, at different ambient temperatures T_f

Compact size (cm)	Dimensionless time relative to the 5 cm compact, $\tau(5\text{ cm})$		
	$T_f = 1370^\circ\text{C}$	$T_f = 1330^\circ\text{C}$	$T_f = 1290^\circ\text{C}$
0.5	311	848	2340
1	287	835	2300
3	329	750	2241
5	662	930	2213
7	1148	1387	2383
10	2170	2391	3176

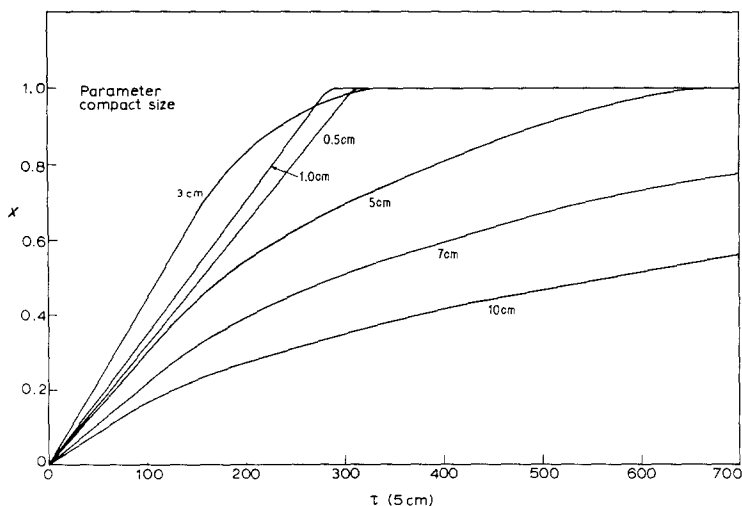


Figure 6 The effect of compact size on the nitridation kinetics, with $T_f = 1370^\circ \text{C}$.

the gas-particle reaction is the rate-controlling factor. Beyond this the flow of gas into the compact begins to play an increasingly important part in the reaction, with the curvature of the lines becoming more pronounced from the increase in temperature gradient. Atkinson, Leatt and Moulson [6] also investigated the effect of changing compact size, presenting their experimental results on a similar graph to Fig. 6. Over the small range of sizes considered 0.3 → 5 cm diameter, they deduced that compact size was an unimportant variable in the nitriding process. This is true for small sized compacts, as the total nitridation time is only affected slightly by small changes in compact size as seen in Figs. 6 and 7.

Table II shows that, for a given T_f , the total reaction times initially decrease and then increase as the compact size is increased. This indicates

the position of the change over from the reaction between silicon and nitrogen as being the rate-determining step, to the gas permeation coming into effect, and also shows how this changes with ambient reaction temperature. The size of compact where this change occurs increases slightly as T_f is decreased, as can be seen by comparing Figs. 6 and 7.

The above results give strong evidence for the existence of a critical compact size for the onset of gas-flow control. This is supported by an elementary mathematical analysis performed by Atkinson *et al.* [6] which also gave a critical compact size of 4 cm for their reaction.

3.3. Arrhenius curves

The rates of conversion for the various temperature runs are compared at constant amounts of

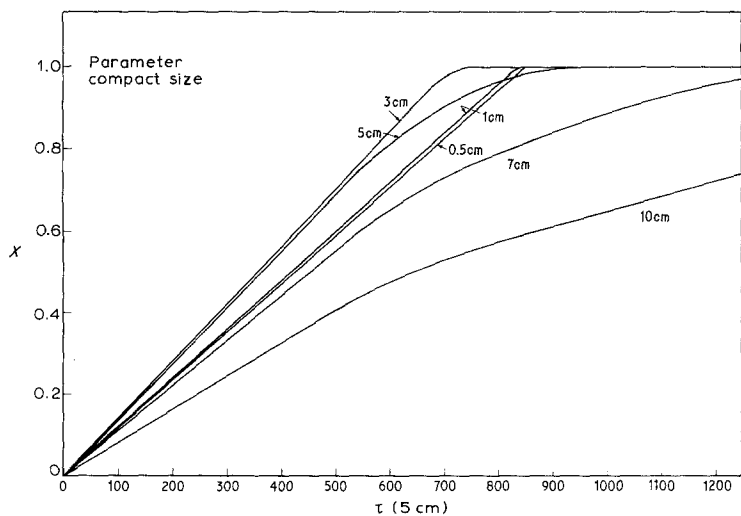


Figure 7 The effect of compact size on the nitridation kinetics, with $T_f = 1330^\circ \text{C}$.

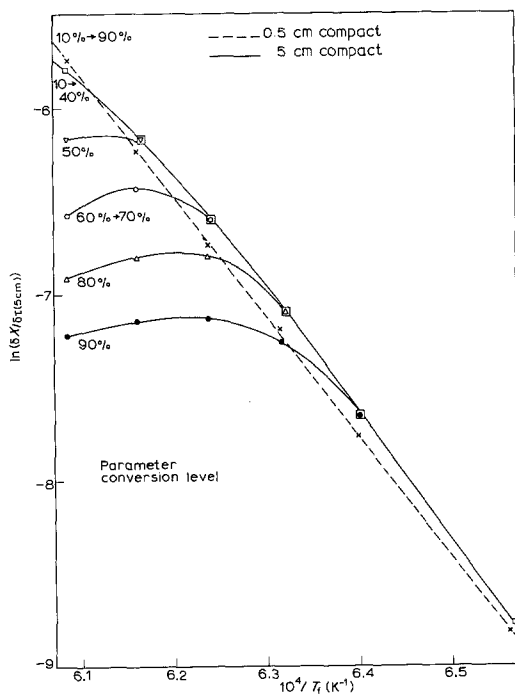


Figure 8 Arrhenius plots of nitridation rates of 5 cm and 0.5 cm compacts.

conversion and Arrhenius plots drawn and presented in Fig. 8 for a 5 cm and a 0.5 cm diameter compact.

We note that the Arrhenius Equation 9 cannot be obtained directly from Equations 3, 4 and 7 without making the assumption that the gas concentration and temperature are constant across the compact. For small compacts this assumption is not unreasonable, as Table I and Figs. 4 and 5 show, the temperature gradients inside the compact are quite small and there is an abundance of nitrogen throughout. But as a is increased, the temperature gradients increase and the reaction becomes diffusion limited. Furthermore, the paper by Atkinson, Leatt and Moulson [6] states that if the gas-particle reaction is the rate-determining step then the dependence of the conversion rate on the temperature should follow an Arrhenius equation. If this is the case, the previous section shows that this would only be applicable to very small compacts anyway.

The temperature used for the Arrhenius plots in [6] was the ambient reaction temperature T_f . For small compacts the maximum temperature attained inside the compact (T_{max}) is only fractionally higher than T_f , and thus the temperature in the Arrhenius equation could be taken as

T_f , for a reasonable approximation. However, as a increases $T_{max} - T_f$ increases, and we can no longer specify "a single temperature" for the reaction. Furthermore, examination of the curves presented in Fig. 8, for which T_f was also used, corroborates the above arguments. As expected the results for the 0.5 cm compact give a reasonably straight line Arrhenius plot, but as the size of the compact is increased above this the straight lines eventually disappear and Equation 9 no longer holds.

The thermal activation energy E , can be calculated from the Arrhenius plots using a least square analysis. Atkinson *et al.* [6] obtained a wide range of values for E using this method, which seems to be a reflection of the fact that the Arrhenius Equation 9 is inappropriately used, as is indicated by the deviation of the curves in Fig. 8 from the straight line.

4. Summary

(a) The maximum temperature observed at the centre by the model and the variation of temperature distribution with time, compare favourably with previous experimental research. However, the temperature rises attained in the compact are found to be dependent on ambient reaction temperature in the range 1250 to 1370° C, contrary to previous deductions [5].

(b) Increasing the ambient reaction temperature accelerates the reaction and at high temperatures, around 1370° C, the reaction begins to show signs of becoming diffusion limited, for the 5 cm compact.

(c) As the compact size increases the resultant temperature rise does not increase without limit, as the permeation of nitrogen into the compact becomes an increasingly important factor for larger compacts.

(d) The evidence obtained points to the existence of a critical compact size for the onset of gas flow control; this critical size is also dependent on the ambient reaction temperature.

(e) The analysis shows that the Arrhenius relationship, Equation 9 proposed, is only applicable to compacts of small size for this reaction, and no analogies from this to larger compacts can be drawn.

References

1. A. J. MOULSON, *J. Mater. Sci.* **14** (1979) 1017.
2. A. ATKINSON, A. J. MOULSON and E. W. ROBERTS, *J. Amer. Ceram. Soc.* **59** (1976) 285.

3. B. S. SAMPATH, P. A. RAMACHANDRAN and R. HUGHES, *Chem. Eng. Sci.* **30** (1975) 125.
4. *Idem*, *Can. J. Chem. Eng.* **53** (1975) 184.
5. A. ATKINSON and A. D. EVANS, *Trans. Brit. Ceram. Soc.* **73** (1974) 43.
6. A. ATKINSON, P. J. LEATT and A. J. MOULSON, *Proceedings of the British Ceramic Society* **22** (1973) 253.
7. R. ARIS in "The Mathematical Theory of Diffusion and Reaction in Permeable Catalysts" (Clarendon Press, Oxford, 1975) Vol. 1.
8. F. L. RILEY, NATO Advanced Study Institute of Applied Science, Nordhoff International Publication **23** (1977) 265.
9. G. S. HUGHES, C. MCGREAVY and J. H. MERKIN, *Can. J. Chem. Eng.* **57** (1979) 198.
10. G. S. HUGHES, Internal Report "Transport effects in non-catalytic gas-solid reactions", University of Leeds (1979).
11. P. J. LEATT and A. J. MOULSON, Progress Reports. M.O.D. (Navy Dept.) 1 (1970); 8 (1971); 9 (1972).
12. S. WHITAKER in "Fundamental principles of heat transfer" (Pergamon Press, Englewood Cliffs 1977) p. 446.

Received 17 December 1979 and accepted 18 February 1980.